PCCP

Accepted Manuscript

ROYAL SOCIETY OF CHEMISTRY

www.rsc.org/pccp

A computational study on the complexation of Np(V) with N,N,N',N'-tetramethyl-3-oxa-glutaramide(TMOGA) and its carboxylate analogs

Jinghui Zeng[1,2], Xia Yang[2], Jiali Liao[1,*], Ning Liu[1], Yuanyou Yang[1], Zhifang Chai[2,3], Dongqi Wang[2,*]

[1] Key Laboratory of Radiation Physics and Technology, Ministry of Education; Institute of Nuclear Science and Technology, Sichuan University, Chengdu, 610064, China

[2] CAS Key Laboratory of Nuclear Radiation and Nuclear Energy Techniques, Institute of High Energy Physics, Chinese Academy of Sciences, Beijing, 100049, China

[3] School of Radiation Medicine and Interdisciplinary Sciences (RAD-X), Soochow University, Suzhou 215123, China

Email: dwang@ihep.ac.cn (D.Wang), liaojiali@scu.edu.cn (J.Liao)

Abstract

Density functional theory has been used to study the geometries and relative stabilities of the complexes of NpO_2^+ with the title compounds (L), including TMOGA, deprotonated N,N'-dimethyl-3-oxa-glutaramic acid (DMOGA) and their deprotonated oxydiacetic analog (ODA). Our calculations suggest that the complexes where the ligands appear as tridentate chelators are more stable than as bidentate ones, and the substitution of the amide group by carboxylate favors the formation of the complexes. Thermodynamically the 1:2 complex (Np-L_2) is more favorable than the 1:1 complex (Np-L) in the cases of TMOGA and DMOGA, but not for ODA anion. Taking into account the solvation effect of water, the 1:2 complex is more favorable than the 1:1 complex for all of the three ligands, though the reaction enthalpy decreases compared to that in the gas phase, and the formation of Np-$(TMOGA)_2$ from Np-TMOGA is roughly a thermal neutral process. The strength of the Np=O bond is weakened upon the coordination of ligands to Np(V) and the increase of the negative charge on the ligand (-1e for deprotonated DMOGA and -2e for deprotonated ODA). The Quantum Theory of Atoms-in-Molecules (QTAIM) was used here to analyze the bonding mode of NpO_2^+-L_x(x=1,2) and to compare the bond order data.

INTRODUCTION

Nuclear energy has been proposed to be one of the future solutions to the energy problem. In the spent nuclear fuel (SNF)[1] taken out of a typical light water reactor, which is not capable of making well use of the fuel, there are substantial fissile materials, either due to the incomplete combustion of the fuel, or generated during an operational period of the reactor. These materials may be recycled for efficient energy production,[2] which stresses the importance of proper reprocessing of the spent fuel in order to nurture a sustainable application of nuclear energy. To recover the actinides and fission products in the spent fuel, a various protocols have been developed during the past decades, such as PUREX,[2-4] TRPO,[5-7] UREX+,[8-11] and the optimization of these existing protocols and the design of new ones are in progress towards the development of advanced SNF reprocessing recycling in which precise control of the element flow is a major topic and challenges nuclear scientists around the world.[8]

Precise control of some actinides, neptunium (Np) in particular, has proven difficult because of its unique properties and behaviors in condensed phase. Np can exist in multiple oxidation states (*i.e.* III, IV, V, VI and VII) and the most stable one in aqueous solutions is Np(V), which has an electronic configuration[12,13] of $[Rn]5f^2$ and appears as neptunyl (NpO_2^+). Neptunyl ion does not form stable complexes with many ligands, leading to its very low extractability in solvent extraction separation processes.[8,12,14]

In recent years, oxy-[12,15,16] and nitrilo-[8,12,14] dicarboxylic acids and their diamide derivatives (e.g. diglycolamides[17] which contains an ether linkage between two amide groups) have been developed as alternatives to the traditional extractants,[5,8,12,14-17] and proved to be able to form moderately strong complexes as tridentate ligands coordinated to NpO_2^+, according to previous experimental studies.[12,14-17] The products, due to the degradation of amides either via radiolysis and/or hydrolysis, are less detrimental to the separation processes, and the presence of alkyl groups in the amide-containing organic ligands also make it relatively easy to strip actinides.[16] In addition, considering the issues of environmental protection and human health, the amides consist of only C, H, O and N which could be completely incinerable so that

the amount of secondary wastes generated in nuclear waste treatment could be significantly reduced.[8,12,14-16] These advantages make this series of extractants a better alternative than traditional organophosphorus compounds in actinide partitioning,[18] which has been illustrated by the application of *N,N′*-dimethyl-3-oxa-glutaramic acid (DMOGA) in the simplification of TRPO process.[5]

Extensive experimental studies[5,8,12,14-17] on the optical properties and structural aspects of these complexation reactions with NpO_2^+ have been reported to address the possible speciation of neptunyl in the presence of the above-mentioned extractants. In their previous study, Rao and Tian investigated[14] a series of structurally related ligands, including *N,N,N′,N′*-tetramethyl-3-oxa-glutaramide (TMOGA), *N,N′*-dimethyl-3-oxa-glutaramic acid (DMOGA) and the dicarboxylate analog-oxydiacetic acid (ODA), which are shown in Scheme 1. In that work,[14] the nitrilo-dicarboxylates were found to form stronger complexes with Np(V) than oxy-dicarboxylates due to a much more favorable enthalpy of complexation. A recent work[19] to mimic the radiolysis of diglycolamide complexes of uranyl, neptunyl and plutonyl in gas phase by means of electrospray ionization and DFT (LDA and PBE) methods shows that C-O^{ether} bond breaks for all of the three complexes, with Np(VI) and Pu(VI) highly possible to be reduced while U(VI) not.

Thermodynamic quantities governing the complexation of actinides with oxa-diamides thermodynamic parameters, *e.g.* enthalpy and entropy, and structural factors, *e.g.* denticity and steric hindrance, that affect the binding strength, are important in understanding the speciation of neptunyl ion.[2,12,14,17] Rao et al.[16] measured the stability constants, enthalpy and entropy of NpO_2^+ complexation using microcalorimetry and spectrophotometry, and found that these properties generally decrease in the order ODA > DMOGA >TMOGA (Scheme 1). This suggests that the substitution of the carboxylate group by an amide group reduces the stability of complexes, which has been attributed to the loss of entropy, the driving force according to Rao et al.,[16] in the complexation process of neptunyl ion to the three ligands.

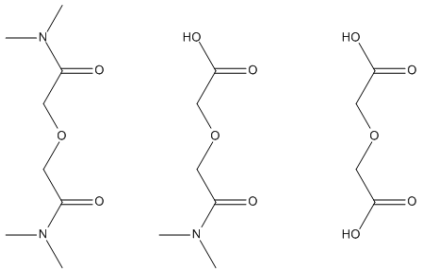

Scheme 1 Chemical structures of TMOGA (left), DMOGA (center), and ODA (right).[16]

As an f^2 electronic system, the absorption bands of Np(V) in the near IR region originate from f-f transitions which are forbidden by Laporte's rule,[8,12,14-16] and a complex with Np as the inversion centroid is "silent" at the band of f-f transitions.[15] Previous X-ray absorption studies in aqueous phase indicate that neptunyl interacts with five H_2O molecules in its first solvation shell, leading to a lack of an inversion center and displaying two f-f transition bands at 980 and 1024 nm.[20,21] The intensive absorption band at 980 nm of hydrated NpO_2^+ cation is widely used in the studies of its complexation with various ligands,[8,12,14-16] both on the determination of Np(V) concentration in solution and the formation of Np(V) complexes[12] for the sensitivity of its intensity and position to the coordination environment of NpO_2^+.

Earlier single-crystal X-ray crystallographic studies[12,15,22] and EXAFS have indicated a centrosymmetric geometry for the NpO_2^+–L_2 (L=ODA, TMOGA) complexes, suggesting that photometric measurement may be inappropriate to capture the feature on the speciation of neptunyl ion in the presence of these ligands in condensed phase. Furthermore, available experimental data reported the formation of 1:1 complex but not the 1:2 one for DMOGA for unclear reasons, despite efforts paid in the experimental studies, and the authors clearly indicated that the unexpected result required further exploration.[16] These open questions remaining to be addressed motivated us to conduct the present quantum chemistry study with the hope to complement experimental studies.

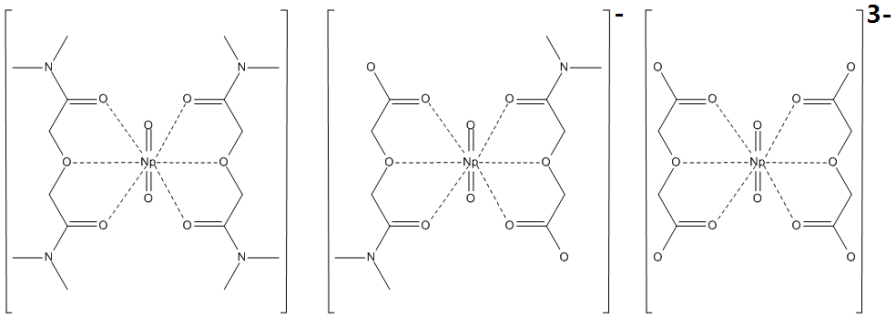

Scheme 2 The possible 1:2 binding mode of NpO_2^+ with ligands: $[NpO_2^+–(TMOGA)_2]$(left), $[NpO_2^+–(DMOGA)_2]^-$(center) and $[NpO_2^+–(ODA)_2]^{3-}$(right)

Though the experimental studies have contributed to the understanding on the coordination of neptunyl ion with ligands by measuring the thermodynamics of the complexation reaction, such as stability constant, enthalpy and entropy, and crystallizing the coordination complexes, they only provide macroscopic information with limited microscopic insights of neptunyl and its complexes on the molecular scale. Computational tools have proved to useful in providing details of electronic and molecular structure and mechanistic information on reactions at the molecular level, which complements experimental studies of actinide-containing systems.[23-30]

Computational studies concerning the speciation of neptunyl ion in the presence of organic ligands in condensed phase are rare, and one of the few studies compares[31] the coordination of uranyl and neptunyl to carbamoylmethylphosphine oxide ligand (CMPO) using DFT method, and found that CMPO and Ph_2CMPO ligands have higher selectivity for UO_2^{2+} over NpO_2^+, and for all of the extraction complexes, the metal–ligand interactions are mainly ionic. They also proposed that hydration energies might play an important role in the extractability of CMPO and Ph_2CMPO for these actinyl ions.

The present study concerns the interaction between neptunyl and TMOGA and its carboxylate analogs. We have employed DFT method to investigate the possible coordinate modes and the bond features in these complexes, through which we hope to contribute to the understanding on the molecular mechanisms on the extraction of neptunyl ion.

METHODOLOGY

The molecular systems in experimental studies,[16] TMOGA, DMOGA and ODA, were used as the prototype models. A set of possible coordination complexes, where the ligands may present as bidentate or tridentate ligands, have been prepared and fully optimized using B3LYP[32,33] functional to identify the most probable coordination mode of neptunyl cation to the three ligands. This functional is reported to give similar results to CCSD(T) in view of geometry,[34,35] while large deviations may be found in energy calculations from that of high level correlated wave function methods.[35]

The small-core (5f-in-valence) effective core potential (ECP) of Dolg et al.[36-38] was used for Np, with 60 core electrons and 33 electrons in the valence shell, and a contraction scheme of (14s13p10d8f6g)/[10s9p5d4f3g] was used for the basis set to represent the outer shell electrons of Np atom.[36,37] For all the other atoms, including C, N, O and H, 6-31G(d)[39] basis set was used. This combination is denoted as BS1. SCF procedure was set to quadratically convergent[40] and no symmetry constraint was imposed. The default integration accuracy in Gaussian09, FineGrid, was used in the calculations.

Frequency calculations were performed to verify the nature of each optimized stationary structure and to abstract the thermodynamic quantities of each species. The Quantum Theory of Atoms in Molecules (QTAIM)[35,41-44] analysis was performed based on Kohn-Sham orbitals optimized by the Gaussian program. Solvent effect was taken into account with the SMD model[45] as implemented in the Gaussian 09 package[46], which was used to conduct all of the optimizations and vibrational analyses, GaussView 5.0 package[47] to view the vibrational modes of optimized stationary points and prepare for the graphics. The AIM analysis was done using Multiwfn 3.2 package.[48]

To refine the energies, another combination, BS2, was used with all atoms other than Np treated by 6-311++G** in single point calculations using B3LYP and CCSD(T) method. For comparison, additional calculations at CCSD(T)/BS1 level

were also carried out. All data discussed here are from calculations in aqueous phase using SMD model at the level of B3LYP/BS1 unless stated otherwise， and all the other data, including optimized atomic coordinates and absolute energies, are provided in ESI.

RESULTS AND DISCUSSION

A. Geometries and relative energies.

A various coordination modes of ODA, DMOGA and TMOGA to NpO_2^+ have been evaluated using B3LYP functional, and the complexes may form with a stoichiometric ratio of Np:L=1:1 or 1:2. For the three ligands, we have considered TMOGA as a tridentate ligand, while ODA and DMOGA as either tridentate or bidentate ligands. The optimized structures of the complexes with the lowest energies obtained from the calculations in aqueous phase are shown in Figure 1, both in the stoichiometry of 1:1 and 1:2 for M:L, and key geometric parameters and the binding energetics are given in Tables 1 and 2.

Since the two O^{yl} atoms occupy the axial position, as seen in Figure 1, ligands interact with Np in the equatorial plane, where Np atom is able to accommodate 5 or 6 electron donors. In the M:L=1:1 complexes, the ligand takes two or three coordinate sites, and the unoccupied sites may be filled by water molecules or other electron donors. In Rao's experiment,[16] sodium perchlorate was used to attain a constant ionic strength. As ClO_4^- is known as a poor complexing anion,[49] we consider only the complexes with water, the organic ligand or both of them.

A.1 Geometry.

Experimental studies have crystallized a 1:2 complex of neptunyl and ligand where the ligand is ODA[15] or TMOGA[22], while a 1:1 complex for DMOGA,[16] and it is hypothesized that in aqueous phase an equilibrium may exist between the 1:1 and 1:2 complexes. According to our calculations, both the 1:1 and 1:2 complexes are energetically stable in gas phase and in aqueous phase, and the optimized structures of these key species are shown in Figure 1.

TMOGA. As seen in Figure 1.T1, in the 1:1 complex, the ligands occupy three

equatorial sites, and water for the other two. In the naked neptunyl cation, the distance of Np-O^{yl} is calculated to be 1.74 or 1.82 Å in the gas phase and in the aqueous phase respectively. The explicit treatment of five water molecules in the first solvation shell leads to a marginal increase of the Np-O^{yl} distance by 0.04 or 0.01 Å, respectively (see SI). The addition of one more water molecule, i.e. six water molecules in the equatorial plane in total, brings a negligible effect with an increase of 0.01 Å both in the gas phase and in the aqueous phase. Meanwhile in the presence of six water molecules, two of them actually have very weak interaction with Np with a distance of 3.75 Å in aqueous phase treated by SMD model. In other words, in aqueous phase, neptunyl ion may accommodate 5 water molecules in the first solvation shell, and the excess solvent molecules assembly in the outer solvent shells. These observations qualify a model system with a coordination number of 5 in the equatorial plane of neptunyl ion.

Figure 1 depicts the optimized structures of $[NpO_2(TMOGA)(H_2O)_2]^+$ (T1) and $[NpO_2(TMOGA)_2]^+$ (T2). In T1 complex, the two O^{amide} atoms show stronger interaction with Np (distances are 2.48 – 2.50 Å in gas phase and about 2.56 - 2.57 Å in aqueous phase) than the O^{ether} atom (distance 2.70 - 2.72 Å). The presence of a second TMOGA weakens the strength of the coordination bond in aqueous phase (distances of 2.59-2.66 Å between Np and O^{amide} and of 2.98 Å between Np and O^{ether}). This indicates a stronger coordination of Np to TMOGA than to water, implying a more favorable binding of Np to TMOGA than to water in aqueous phase.

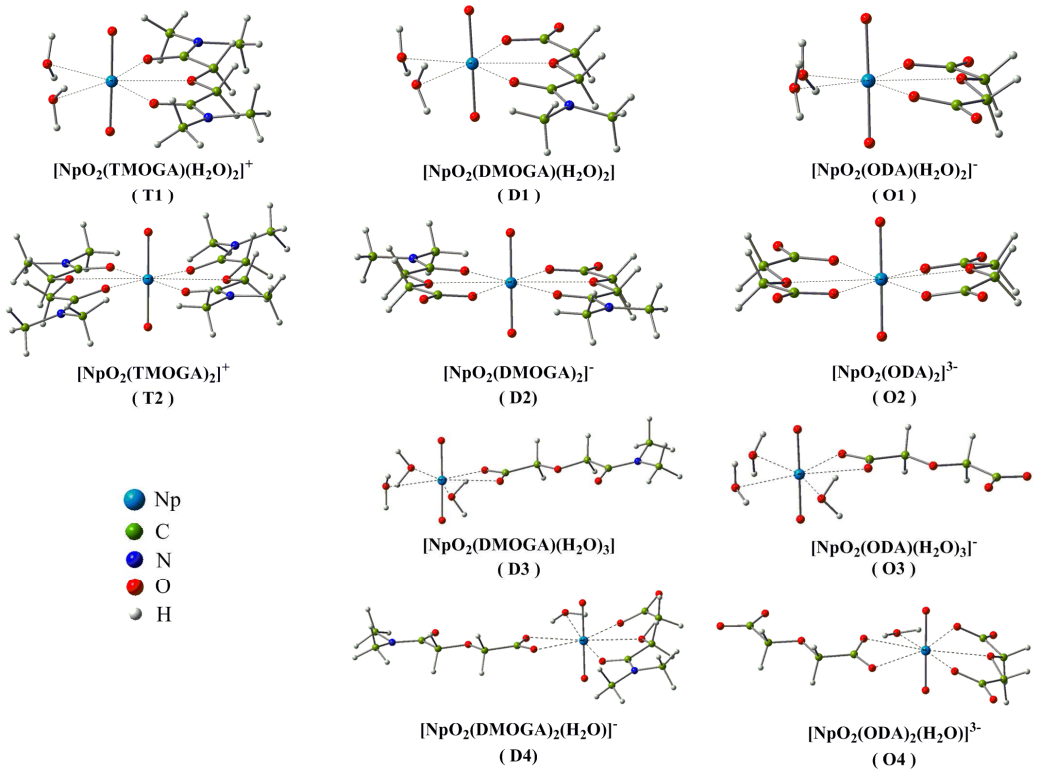

Figure 1 The geometries of $Np(H_2O)_nL_m$ (n=1-3, m=1,2) complexes optimized in aqueous phase using SMD continnum model at B3LYP level.

Table 1 The calculated Np-O distances (*d*, in Å) and the corresponding Mayer bond order (MBO) in aqueous phase by SMD model[(a)]

	O^{yl}		O^{amide}		O^{ether}		O^{carb}		O^{water}	
	d	MBO	*d*	MBO	*d*	MBO	*d*	MBO	*d*	MBO
T1	1.82	2.03	2.57	0.30	2.72	0.16	-	-	2.74	0.29
D1	1.83	2.02	2.54	0.31	2.67	0.18	2.48	0.42	2.68-2.72	0.29
O1	1.84	2.01	-	-	2.73	0.18	2.54	0.39	2.63-2.65	0.29
T2	1.83	2.01	2.59-2.66	0.27-0.29	2.98	0.12	-	-	-	-
D2	1.84	2.00	2.74	0.25	2.95	0.14	2.59	0.36	-	-
O2	1.85	1.99	-	-	2.83-3.00	0.13-0.16	2.58-2.62	0.35-0.36	-	-
D3	1.83	2.03	-	-	-	-	2.60-2.61	0.34	2.60-2.70	0.29-0.31
O3	1.84	2.02	-	-	-	-	2.61-2.70	0.32-0.34	2.62-2.84	0.26-0.30

[(a)]: see Figure 1 for the conformations of the complexes.

DMOGA. The substitution of one amine group of TMOGA by a carboxylate group gives DMOGA. This endows the ligand the ability to adopt two coordination

modes when interacting with the central metal cation, as seen in Figure 1.D1, where DMOGA appears as a tridentate ligand; and in Figure 1.D3, where the carboxylate group of DMOGA interacts with Np atom. To saturate the coordination of Np in the equatorial plane and to make a fair comparison on the strength of the coordination modes, in the former case, two water molecules were taken into account, while in the latter case, there are three water molecule, thus in both cases Np atom receives 5 electronic donor in the equatorial plane. In view of geometric parameters, it is hard to judge the priorities of the coordination modes given the essentially same Np-O^{yl} and Np-O^{water} distances and Mayer bond orders (see Table 1), and binding energies should be used to evaluate the strength of different coordination modes.

ODA. As mentioned above, same as DMOGA, ODA may appear as a bi- or a tridentate ligand. Meanwhile, due to the doubly substitution of the terminal amine groups of TMOGA by a charged carboxylate group, the ODA ligand carries -2e charge, and is able to build up stronger electrostatic interactions with the positively charged neptunyl ion. This perturbs the Np-O^{yl} interaction and makes the bond length increase by 0.02 Å compared to the TMOGA case in the 1:1 complex.

A.2 Energy.

In order to understand the speciation of neptunyl ion in the presence of the three ligands, we have considered the complex formation reactions shown in Schemes 3-5. The relative free energies calculated in gas-phase and in aqueous phase, ΔG_g and ΔG_{aq}, are tabulated in Table 2.

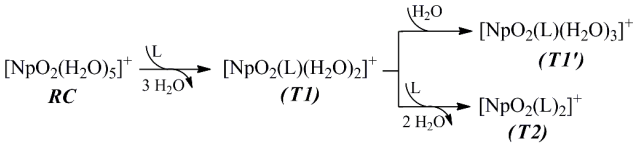

Scheme 3 The complexation of hydrated neptunyl with TMOGA (L)

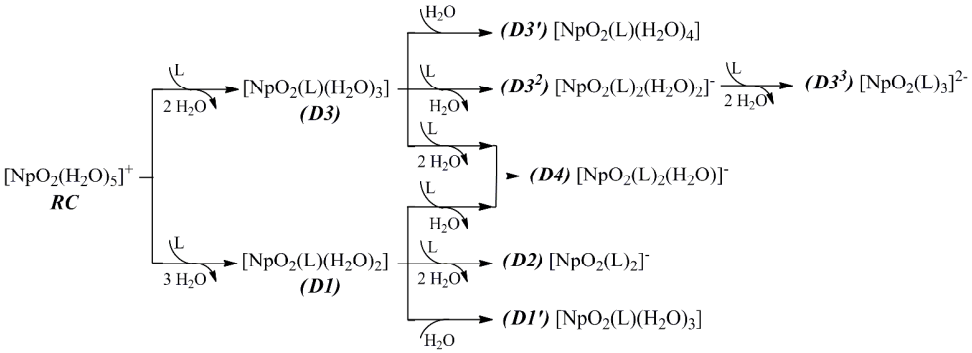

Scheme 4 The complexation of hydrated neptunyl with DMOGA (L)

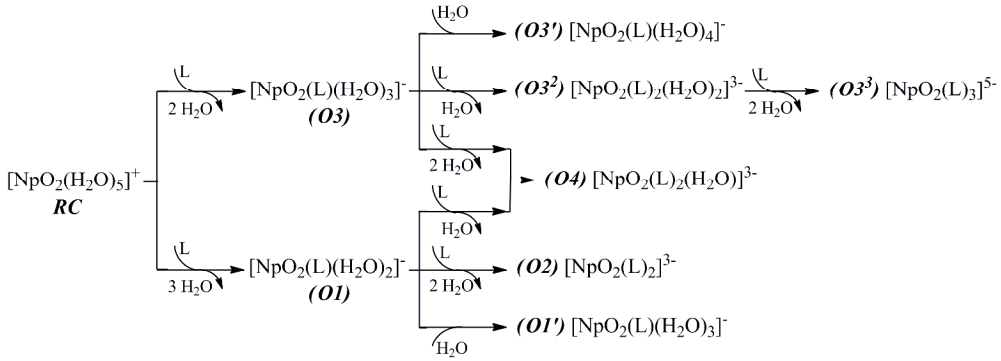

Scheme 5 The complexation of hydrated neptunyl with ODA (L)

Our calculations first verified the probable form of hydrated neptunyl ion in aqueous phase, i.e. as a complex with five water molecules coordinated in the equatorial plane $[NpO_2(H_2O)_5]^+$ rather than $[NpO_2(H_2O)_6]^+$. For the formation of latter via the addition of one water molecule to the former hydrated form, the relative free energy was calculated to be 0.8 kcal/mol (ΔG_{aq}) and 3.7 kcal/mol (ΔG_g) respectively, suggesting the located $[NpO_2(H_2O)_6]^+$ is marginally less stable than $[NpO_2(H_2O)_5]^+$ while more stable in aqueous phase. However, a close check of the geometries of the two complexes shows that the excess stabilization of the former than the latter in aqueous phase comes from the hydrogen bond between water molecules. In the optimized geometries (see SI), the $[NpO_2(H_2O)_5]^+$ holds a pentagonal bipyramidal conformation, while in $[NpO_2(H_2O)_6]^+$, two of the six water molecules are far away, as observed in previous studies of uranyl and neptunyl(VI),[50,51] where the hydration number of hexavalent neptunyl is assigned as 5, and Tsushima[52] and Gagliardi[53] et al.

got same results. This qualifies our study with a penta-coordinated hydrated neptunyl species as the starting complex of the ligand exchange reactions.

The processes included in Schemes 3-5 cover the complex formation reactions starting from hydrated neptunyl to form the 1:1 complex through the exchange of two or three coordinated water molecules by a ligand, either as a bidentate or a tridentate chelate ligand. The complex may then experience the addition of one more water molecule, or another exchange reaction to form the 1:2 complex. When the ligand, either ODA or DMOGA, appears as a bidentate ligand, it is possible for a third ligand to attach to Np to form a M:L=1:3 complex.

Note that in our calculations, we have considered the deprotonated forms of the ligands, i.e. the ligands carry 0e, -1e and -2e charge on TMOGA, DMOGA and ODA, respectively. The distinct charge states of the ligands have different atomic charge distribution (Mulliken atomic charges on O^{ether} and the two O^{carb} atoms are calculated with SMD model to be [-0.53, -0.63, -0.63], [-0.53, -0.70, -0.63] and [-0.53, -0.70, -0.70], respectively in TMOGA, DMOGA and ODA) which can certainly affect their ability to bind to Np atom. According to our calculations, as a tridentate ligand, the bind of TMOGA to Np(V), which releases three water molecules, is an exothermic process by 13.9 kcal/mol. This value becomes 18.7 and 33.8 kcal/mol for DMOGA and ODA, respectively. The addition of a second ligand is a thermal neutral process for TMOGA, while brings further stabilization along the reactions in the case of the latter two ligands by 14.9 and 6.7 kcal/mol, respectively. The trend is consistent with the experimental data measured by Rao et al.,[16] which indicates that the ligand bearing carboxylate group is energetically more favorable for the complexation of neptunyl.

Table 2 The calculated relative enthalpy (kcal/mol), entropy (kcal/mol), free energy (kcal/mol) of the complexes at 298.15 K in gas phase and aqueous phase.

Complexation reactions[(b)]	gas			aq.[(a)]			Expt.	
	ΔH	*T*ΔS	ΔG	ΔH	*T*ΔS	ΔG	ΔH	*T*ΔS
(1) $[NpO_2(H_2O)_5]^+$ +TMOGA→ T1+3(H_2O)	-5.5	18.1	-23.6	3.4	17.3	-13.9	1.1[(c)]	3.0[(c)]
(2) T1 + TMOGA → T2 + 2(H_2O)	-15.8	4.2	-20.0	3.2	3.1	0.1	9.3[(c)]	10.8[(c)]

(3) $[NpO_2(H_2O)_5]^+$ +DMOGA→ D1+3(H_2O)	-101.0	13.9	-114.9	-3.9	14.9	-18.7	1.3[(c)]	5.3[(c)]
(4) D1 + DMOGA → D2 + 2(H_2O)	-28.4	4.6	-33.0	-9.0	5.9	-14.9	-	-
(5) $[NpO_2(H_2O)_5]^+$ +DMOGA→ D3+2(H_2O)	-111.3	6.5	-117.8	-2.2	6.7	-8.9	-	-
(6) $[NpO_2(H_2O)_5]^+$ +ODA→ O1+3(H_2O)	-202.9	12.8	-215.6	-18.8	15.1	-33.8	2.1[(d)]	7.3[(d)]
(7) O1 + ODA → O2 + 2(H_2O)	80.9	7.7	73.2	-2.4	4.3	-6.7	-	-
(8) $[NpO_2(H_2O)_5]^+$ + ODA→ O3+2(H_2O)	-174.6	5.7	-180.3	-11.5	7.5	-19.0	-	-
(9) $[NpO_2(H_2O)_5]^+$ +MIDA→ M1+3(H_2O)	-200.8	12.6	-213.3	-17.2	16.4	-33.5	-4.0[(e)]	6.0[(e)]
(10) M1 + MIDA → M2(trans) + 2(H_2O)	88.3	8.9	79.4	1.0	5.0	-4.1	-1.3[(e)]	0.9[(e)]
(11) M1 + MIDA → M2(cis) + 2(H_2O)	96.5	8.8	87.7	7.8	3.6	4.2	-	-
(12) $[NpO_2(H_2O)_5]^+ + H_2O → [NpO_2(H_2O)_6]^+$	-11.7	-12.5	0.8	-14.8	-11.0	-3.7	-	-

[(a)]: Solvent effect was taken into account using SMD model.

[(b)]: T1: $[NpO_2(TMOGA)(H_2O)_2]^+$, T2: $[NpO_2(TMOGA)_2]^+$, D1: $[NpO_2(DMOGA)(H_2O)_2]$, D2: $[NpO_2(DMOGA)_2]^-$, D3: $[NpO_2(DMOGA)(H_2O)_3]$, O1: $[NpO_2(ODA)(H_2O)_2]^-$, O2: $[NpO_2(ODA)_2]^{3-}$, O3: $[NpO_2(ODA)(H_2O)_3]^-$, M1: $[NpO_2(MIDA)(H_2O)_2]^-$, M2(trans/cis): $[NpO_2(MIDA)_2]^{3-}$.

[(c)]: data from ref. 16

[(d)]: data from ref. 54

[(e)]: data from ref. 14

To evaluate the importance of the bridging ether group, we tested another ligand, MIDA, which differs from ODA in the substitution of the O^{ether} atom by a methylated amine group, and the optimized 1:1, 1:2(trans), and 1:2(cis) neptunyl-MIDA complexes are shown in Figure 2. In view of energies (Table 2, reactions (9)-(11)), the replacement of the O^{ether} of the ligand by an amine group brings adverse effect on its coordination to neptunyl cation. As amine is a softer base than the O^{ether} atom, it is conceivable that MIDA does not build stronger interaction with the "hard" acid neptunyl(V) cation.

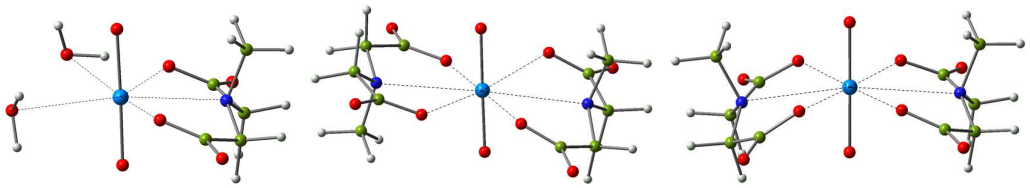

Figure 2 The 1:1 (left), 1:2(trans) (middle), and 1:2(cis) (right) neptunyl-MIDA complexes.

We note that for the ligand exchange reactions where the overall charge of the complexes reduces to near zero along the reaction, e.g. the pathways (3), (5), (6), (8),

and (9) in Table 2, there is large difference in the relative free energies between the values obtained in gas phase and in aqueous phase by SMD model. This is related to the different degree of solvation of the charged reactant and its corresponding product, i.e. $[NpO_2(H_2O)_5]^+$ and $[NpO_2L(H_2O)_n]^{0/-1}$, respectively. In an earlier work of Schreckenbach et al.,[55] large difference in the binding energy of actinide with crown ether in aqueous solution between their +6 and +5 oxidation states was addressed in terms of difference solvation, and they found that the solvation disfavored the ligand exchange reaction of water in hydrated actinyl(VI) by a crown ether more than in the case of actinyl(V) due to the stronger screening of the charge of An(VI) than that of An(V) by the crown ether, which makes the An(V) crown ether complexes more stable. The current case is much simpler. As the stabilization of a charged species, here the hydrated neptunyl and the DMOGA/ODA/MIDA, via the polarization of solvent depends on the charges and the distance between point charge pair, the solvation favors the left side of the ligand exchange reaction more than the right side, leading to much less exothermicity in aqueous phase than in gas phase.

When DMOGA and ODA appear as bidentate ligands, the formation of 1:1 complexes is exothermic by 8.9 and 19.0 kcal/mol, respectively. The addition of a second ligand brings an exothermicity of 5.6 kcal/mol for DMOGA while an endothermicity of 4.5 kcal/mol for ODA (see SI). The presence of a third ligand in the complex is thermodynamically favorable in both cases with energy of 4.2 and 6.3 kcal/mol, respectively (see SI).

The addition of the second ligand may also adopt a tridentate chelation mode. According to our calculations, such a coordination mode brings substantial exothermicity by 15.9 and 15.4 kcal/mol (see SI), respectively, which suggests a much stronger preference for the ligand to coordinate to Np via a tridentate chelation mode.

B. QTAIM analysis

The Kohn-Sham orbitals obtained in geometry optimization calculations were used to calculate the electron density of the complexes and perform the QTAIM topology analysis of Bader[41,44] and Mata and Boyd[42] et al., which focuses on molecular electron density rather than orbital structure. There are examples[56,57]

showing that the contribution of 5f orbital in actinide complexes may be overestimated in molecular orbital analysis based on density functional theory compared to experimentally determined results, which casts doubt on the reliability of characterization of covalency of the bonding interaction between actinide and ligand. AIM provides an alternative way to study the nature of chemical bond.

Four descriptors in the concept of AIM, i.e. the electron density ρ_b at the bond critical point (BCP), the Laplacian of electron density at BCP ($\bigtriangledown^2\rho_b$), the delocalization index (*DI*(A,B)), the total energy density at BCP (H_b), have been used to characterize the interaction between Np and the ligands. BCP corresponds to the minimum of the electron density along the bond path of an atom pair, with which the chemical bonding interactions may be characterized according to the properties of electron and energy densities. In a naked neptunyl ion, the BCP is closer to the *yl*-oxygen (O^{yl}) than to the neptunium atom (see the d_1/d_2-value in Supporting Information, where d_1 and d_2 are the distances between BCP and Np, and between BCP and O^{yl} or O^{L}, respectively). The density ρ_b at BCP is calculated to be 0.335 $e^-/bohr^3$ in gas phase and 0.269 $e^-/bohr^3$ in aqueous solution. According to Bader, based on the analysis of various systems, a ρ_b value of 0.2 $e^-/bohr^3$ may work as the lower bound to judge a covalent bond and a value of 0.1 $e^-/bohr^3$ as an upper bound for closed-shell interactions including ionic interactions.

At the BCP, the gradient of the electron density is zero, while the Laplacian $\bigtriangledown^2\rho_b$ might be positive if there is a depletion of charge at the BCP or negative if there is a localized charge distribution. For a single bond, the latter is a sign of covalent interaction. For a multiple bond, the delocalization index, *DI*(A,B), which integrates the electron density ρ_b in the bonding region between two atoms A and B and can be used as a measure of the bond order, should be used. Note that the computed values are always smaller than what is expected from the Lewis structures.[35,41]

According to our calculations, the value of ρ_b at the neptunyl BCPs is similar to those of the M≡oxo triple bonds.[35,58] The Laplacian at BCP of of Np-O^{yl} bond is 0.24 $e^-/bohr^5$ in aqueous phase and 0.19 $e^-/bohr^5$ in gas phase, and the *DI* value, 2.76 (aq) or 2.86 (gas), suggests a triple bond between Np and O^{yl} in the hydrated neptunyl ion,

which is supported by the calculated Mayer bond order (MBO) of 2.04 (aq) or 2.19 (gas).

When neptunyl ion is coordinated to ligands, either to water or to organic ligands investigated here, there is essentially little build-up of electron density between Np and the electron donor in the first coordination shell, suggesting a dominant contribution of ionic interaction. We note that there is moderately larger accumulation of electron density between Np and O^{amide} than between Np and O^{water}, e.g. in T1, D1 and O1 (see Figure 1 for the structures and SI for the values of electron density). The increasing orbital overlap in the coordination bonds upon the replacement of water molecules in hydrated neptunyl ion by the organic ligands studied here is consistent with the observations above of shorter coordination bond lengths in complexes of neptunyl with TMOGA, DMOGA, and ODA than in pure hydrated neptunyl ion. However, the enhancement in the orbital overlap is not high enough to justify a covalent interaction between Np and the ligand, which is still best described as ionic interaction. In the complexes, the Laplacian is positive with ρ_b-value much smaller than 0.08 $e^-/bohr^3$ calculated for the ionic LiF molecule,[35,41] suggesting only minor electron accumulations between neptunium and the ligands.

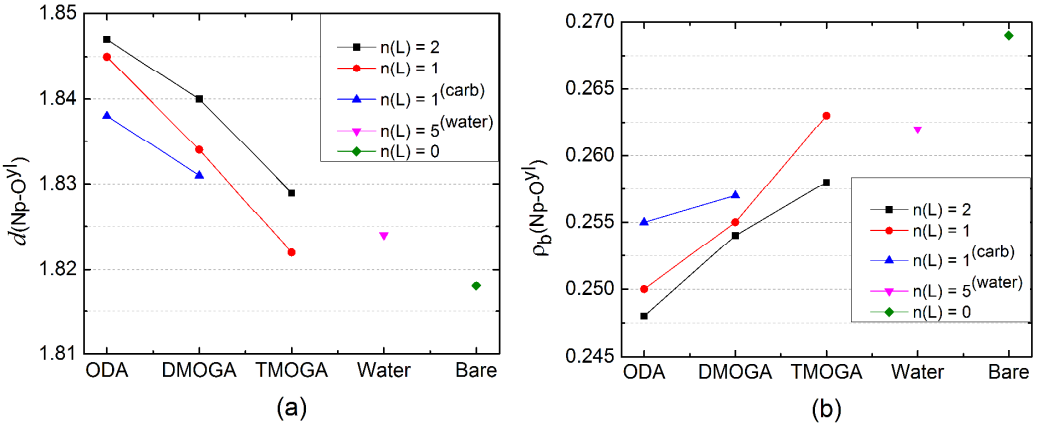

Figure 3 The bond length (Å) *(a)*, and the electron density ρ_b ($e^-/bohr^3$) at BCP *(b)* of Np-O^{yl} bond in NpO_2L_n complexes from calculations in aqueous phase. The values of neptunyl in its hydrated ($NpO_2(H_2O)_n$) and bare forms are also shown for comparison.

In Figure 3 we show how the Np-O^{yl} bond may be perturbed upon the binding of Np to the three ligands. In view of the Np-O^{yl} bond length, the impact due to the coordination of ligands via tridentate chelation mode becomes weaker in the order ODA > DMOGA > TMOGA, and for all of the three ligands, the presence of a second ligand in the complex enhances the perturbation, suggesting stronger binding affinity of neptunyl to all of the three ligands than to water. When DMOGA or ODA works as a bidentate ligand with their carboxylate group, the Np-O^{yl} bond does not feel stronger perturbation even larger contribution of electrostatic interaction is expected, suggesting a higher priority of the ligands to appear as tridentate chelators rather than bidentate ones. The superiority of tridentate chelation may come from the entropic contribution which benefits more from the tridentate chelation mode than from the bidentate one.

The change in the accumulation of electron density in between Np and Oyl atoms is consistent with the above observation. As seen in Figure 2(b), the calculated electron density value increases steadily when going from ODA to TMOGA.

$NpO_2(L)_n(H_2O)_m$	n, m		
TMOGA	1, 2	2, 0	0, 0
DMOGA	1, 2	2, 0	1, 3
ODA	1, 2	2, 0	1, 3

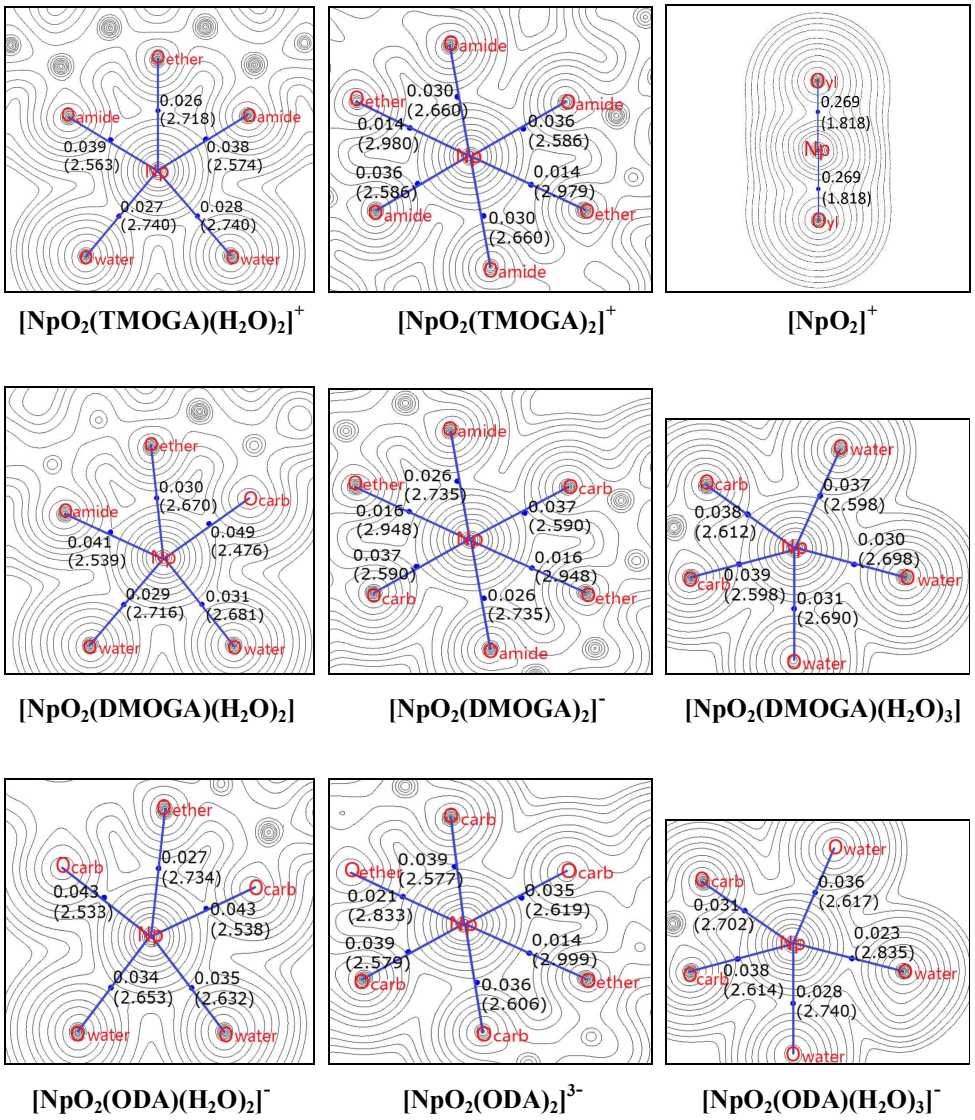

Figure 4 Electron density ρ_b (e^-/bohr^3) and bond length *d* (Å, in parenthesis) of NpO_2^+ complexes from calculations in aqueous phase

In Figure 4, we plotted the electron density and bond length of Np-O bonds in $[NpO_2L_n(H_2O)_m]^{i+}$ (L=TMOGA, DMOGA and ODA, n=1-2, m=2-3). The presence of a second organic ligand leads to a decrease in electron density and an increase of the bond length of Np-O bonds, suggesting stronger *trans* effect of organic ligands than

that of water molecules.

C. A comparison with the experimental work.

It merits a discussion on the consistency and the inconsistency between our calculated results and the experimental data of Rao et al.[16] by means of spectrophotometric/calorimetric titrations. Both studies observe an increase of the stability constants of the complexes, or the free energies of complexation, in the order of TMOGA < DMOGA < ODA, while point to different reasons. In Rao et al.'s work, the enthalpy of complexation was measured to be less endothermic when the ligands vary from ODA to DMOGA to TMOGA by substituting one carboxylate group with an amide group step by step, and entropy was shown to be the driving force for the complexation. In other words, messages delivered by the experimental studies are that the complexation of neptunyl with TMOGA is enthalpically more favorable, while entropically less favorable, compared to the complexation of neptunyl with DMOGA or ODA.

The calculated contributions of enthalpy and entropy to the complexation free energy are plotted in Figure 5. Here we only consider the tridentate coordination mode, and the stoichiometric ratio of both Np:L=1:1 and 1:2. According to our calculations, at the same stoichiometric ratios, the complexations of Np to the three ligands bring similar entropic contribution, while there is large difference in enthalpy change. Enthalpically, the complexation of TMOGA is moderately endothermic, while that of DMOGA or ODA becomes exothermic, suggesting the presence of a negatively charged carboxylate group, being able to build close contact with Np, favors the binding with Np. In regard to the entropy, we consider a comparable entropic contribution being more reasonable concerning that the complexation reactions of the three ligands to Np in the tridentate chelation mode bring similar change in the disordering of the model system, i.e. while the ligand binds to Np, three water molecules are released in all of the three cases. These results indicate that enthalpy and entropy play different roles in the complexation of neptunyl and TMOGA, DMOGA and ODA. For the former one, the entropy is the driving force for

the complexation. For DMOGA, the contribution of enthalpy increases significantly, and becomes competitive against that of entropy in the case of ODA.

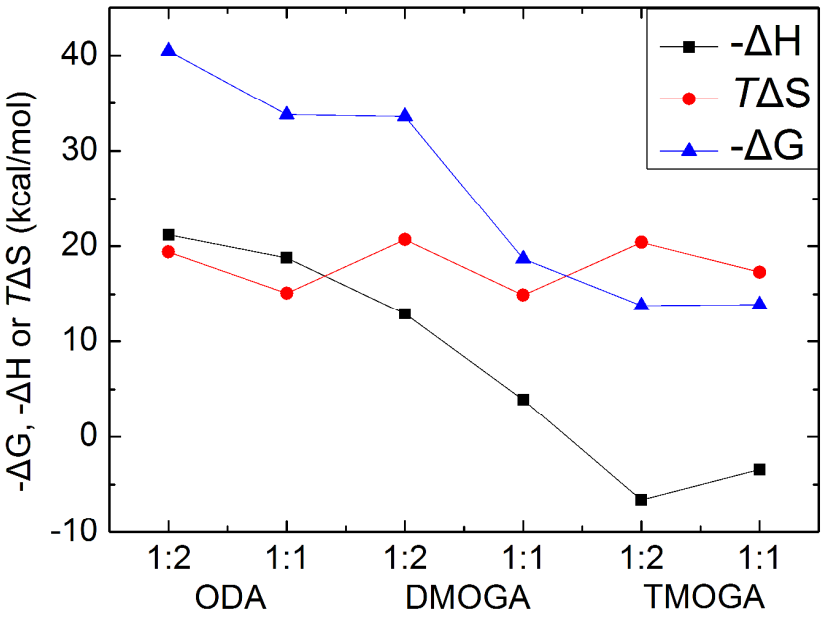

Figure 5 Thermodynamic trends of neptunyl complexes with ODA, DMOGA and TMOGA with a stoichiometric ratio of Np:L=1:1 and 1:2 from calculations in aqueous phase.

As a full geometrical optimization and frequency analysis of the present model systems is beyond our reach, to refine the relative energies, single point energy calculations at the CCSD(T)/BS2 level were carried out and the results are plotted in Figure 6. It is seen that the relative electronic energies of the complexation reactions become negatively larger, while the trend does not change going from ODA to DMOGA and TMOGA.

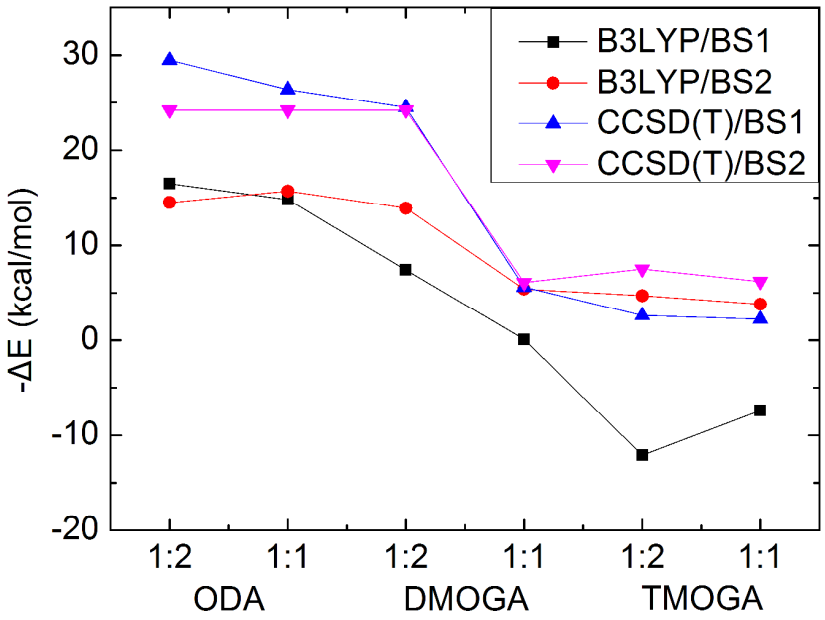

Figure 6 The relative electronic energies of neptunyl complexes with ODA, DMOGA and TMOGA with a stoichiometric ratio of Np:L=1:1 and 1:2 calculated using larger basis set BS2 and/or higher level CCSD(T) method.

We note that Rao et al.[16,59] mentioned that less hydration of the amide group in TMOGA than that of the carboxylate group in ODA or DMOGA made it easier for the carbonyl group of amide to attach to Np than that of carboxylate since less energy was required to dehydrate the carbonyl thus less endothermic enthalpy and smaller entropy of complexation in the case of TMOGA than that of ODA or DMOGA. Indeed the carboxylate group is more hydrophilic than the amide group. However, the opposite charges that neptunyl and DMOGA or ODA carry may bring substantially stronger electrostatic interaction between them than in the case of TMOGA.

Note that the current study was carried out in aqueous phase treated with continuum model, which may suffer from the inadequacy of sampling to evaluate the entropic contribution accurately. Meanwhile, we did not take into account of the screening effect of counterions. Thus, the results represent an ideal case where only the interaction between neptunyl and the TMOGA ligand or its analogs is taken into account in aqueous continuum. This does not allow a direct comparison to the work of Rao et al., while may shed light on the fundamental mechanism of the interaction

between neptunyl and the TMOGA ligand and its analogs, and can therefore contribute to the development of new type functional molecular systems towards efficient extraction of neptunyl.

CONCLUSION

The present study aims at the characterization of speciation of neptunyl ion in the presence of TMOGA, deprotonated DMOGA and ODA.

By comparing the relative energies, bond distances and the total electronic density, the calculations suggest that the complexes where the ligands appear as tridentate chelators are more stable than the bidentate mode, and the substitution of the amide group by carboxylate favors the formation of the complexes, i.e. ODA > DMOGA > TMOGA.

Thermodynamically the 1:2 complex (Np-L_2) is more favorable than the 1:1 complex (Np-L) in the cases of TMOGA and DMOGA, but not for their dicarboxylate analog, oxy-diacetic (ODA) anion, due to the electrostatic repulsive interaction. Taking into account the solvation effect of water, for all of the three ligands, the 1:2 complex is thermodynamically more favorable than the 1:1 complex, and the ligand exchange reaction from Np-TMOGA to Np-$(TMOGA)_2$ is roughly a thermal neutral process. The strength of the Np-O^{yl} bond is weakened upon the coordination of ligands to Np(V) and the increase of the negative charge on the ligand (-1e for deprotonated DMOGA and -2e for deprotonated ODA).

The Quantum Theory of Atoms-in-Molecules (QTAIM) was used here to analyze the bonding mode of NpO_2^+-L_x(x=1,2) and compare to the Mayer bond order data which agree well with the messages delivered by the analysis of geometric parameters and free energies along the ligand exchange reactions.

In summary, our calculations suggest that at the molecular scale, the roles of enthalpic and entropic contributions in the complexation of neptunyl complexes with TMOGA, DMOGA or ODA are different, and the interaction between Np and the electron donor atoms in the first coordination shell is best described as ionic interaction.

ACKNOWLEDGMENTS

This work was financially supported by the National Natural Science Foundation of China to N. Liu (Nos. 91126013 and U1330125), to Z. Chai (No. 91026000), to D. Wang (No. 91226105), and by the Chinese Academy of Sciences in the framework of a Frontier of Novelty program to D. Wang (Nos. Y1515540U1 and Y2291810S3), which are gratefully acknowledged. Calculations were done on the computational grids in the computer center of the Institute of High Energy Physics (IHEP), in the Supercomputing Center of Chinese Academy of Sciences (SCCAS) and in the National Supercomputing Center in Tianjin (NSCC-TJ).

Electronic Supplementary Information

Reaction pathways, geometries of all located stationary points with key geometric and AIM parameters are avilable.

REFERENCE

(1) Bruno, J.; Ewing, R. C. *Elements* **2006**, *2*, 343.
(2) Gorden, A. E. V.; DeVore, M. A. Ⅱ.; Maynard, B. A. *Inorg. Chem.* **2012**, *52*, 3445.
(3) May, I.; Taylor, R. J.; Wallwork, A. L.; Hastings, J. J.; Fedorov, Y. S.; Zilberman, B. Y.; Mishin, E. N.; Arkhipov, S. A.; Blazheva, I. V.; Poverkova, L. Y.; Livens, F. R.; Charnock, J. M. *Radiochim. Acta* **2000**, *88*, 283.
(4) Joshi, J. M.; Pathak, P. N.; Manchanda, V. K. *Solvent Extr. Ion Exch.* **2005**, *23*, 663.
(5) Zhang, P.; Wang, H. R.; Wang, J. C.; Chen, J. *J. Radioanal. Nucl. Chem.* **2007**, *273*, 65.
(6) Zhu, Y. J. *J. Tsinghua University* **1992**, *32*, 1.
(7) Bush, R. P.; Mills, A. L.; Stearn, M. L. Comparison of the plant requirements, process performance and waste arising for potential processes for the partitioning of high level waste. In *Global'95, Intern. Conf. on Evaluation of Emerging Nuclear Fuel Cycle Systems*, The French Section of ANS and the Fuel Cycle and Waste Management Division, Versailles, France, 1995.
(8) Tian, G. X.; Rao, L. F.; Teat, S. J. *Inorg. Chem.* **2009**, *48*, 10158.
(9) Vandegrift, G. F.; Regalbuto, M. C.; Aase, S.; Bakel, A.; Battisti, T. J.; Bowers, D.; Byrnes, J. P.; Clark, M. A.; Emery, J. W.; Falkenberg, J. R.; Gelis, A. V.; Pereira, C.; Hafenrichter, L.; Tsai, Y.; Quigley, K. J.; Vander Pol, M. H. Designing and Demonstration of the UREX+ Process Using Spent Nuclear Fuel. In *Proceedings of ATALANTE-2004 Conference*, Nimes, France, June 21-24, 2004.

(10) Laidler, J. J.; Bresee, J. C. The Advanced Fuel Cycle Initiative of the U.S. Department of Energy: Development of Separations Technologies. In *Proceedings of WM-04 Conference*, Tucson, AZ, February 29 to March 4, 2004.
(11) Vandegrift, G. F.; Regalbuto, M. C.; Aase, S.; Arafat, H.; Bakel, A.; Bowers, D.; Byrnes, J. P.; Clark, M. A.; Emery, J. W.; Falkenberg, J. R.; Gelis, A. V.; Hafenrichter, L.; Leonard, R.; Pereira, C.; Quigley, K. J.; Tsai, Y.; Vander Pol, M. H.; Laidler, J. J. Lab-Scale Demonstration of the UREX+ Process. In *Proceedings of WM-04 Conference*, Tuscon, AZ, February 29 to March 4, 2004.
(12) Rao, L. F.; Tian, G. X. *Symmetry* **2010**, *2*, 1.
(13) Hay, P. J.; Martin, R. L.; Schreckenbach, G. *J. Phys. Chem. A* **2000**, *104*, 6259.
(14) Tian, G. X.; Rao, L. F. *Dalton T.* **2010**, *39*, 9866.
(15) Tian, G. X.; Rao, L. F.; Oliver, A. *Chem. Commun.* **2007**, *(40)*, 4119.
(16) Rao, L. F.; Tian, G. X.; Teat, S. J. *Dalton T.* **2010**, *39*, 3326.
(17) Ansari, S. A.; Pathak, P.; Mohapatra, P. K.; Manchanda, V. K. *Chem. Rev.* **2012**, *112*, 1751.
(18) Raut, D. R.; Mohapatra, P. K.; Ansari, S. A.; Godbole, S. V.; Iqbal, M.; Manna, D.; Ghanty, T. K.; Huskens, J.; Verboom, W. *RSC Adv.* **2013**, *3*, 9296.
(19) Gong, Y.; Hu, H. S.; Rao, L. F.; Li, J.; Gibson, J. K. *J. Phys. Chem. A* **2013**, *117*, 10544.
(20) Allen, P. G.; Bucher, J. J.; Shuh, D. K.; Edelstein, N. M.; Reich, T. *Inorg. Chem.* **1997**, *36*, 4676.
(21) Combes, J. M.; Chisholm-Brause, C. J.; Brown, J. G. E.; Parks, G. A.; Conradson, S. D.; Eller, P. G.; Triay, I. R.; Hobart, D. E.; Meijer, A. *Environ. Sci. Technol.* **1992**, *26*, 376.
(22) Tian, G. X.; Xu, J. D.; Rao, L. F. *Angew. Chem. Int. Ed.* **2005**, *44*, 6200.
(23) Kaltsoyannis, N.; Hay, P. J.; Li, J.; Blaudeau, J. P.; Bursten, B. E. Theoretical studies of the electronic structure of compounds of the actinide elements. In *The Chemistry of The Actinide and Transactinide Elements*. Morss, L. R., Edelstein, N. M., Fuger, J., Katz, J. J., Eds., Springer: Dordrecht, The Netherlands, 2008, p 1893.
(24) Wang, D. Q.; Van Gunsteren, W. F.; Chai, Z. F. *Chem. Soc. Rev.* **2012**, *41*, 5836.
(25) Vallet, V.; Macak, P.; Wahlgren, U.; Grenthe, I. *Theor. Chem. Acc.* **2006**, *115*, 145.
(26) Lan, J. H.; Shi, W. Q.; Yuan, L. Y.; Li, J.; Zhao, Y. L.; Chai, Z. F. *Coord. Chem. Rev.* **2012**, *256*, 1406.
(27) Schreckenbach, G.; Hay, P. J.; Martin, R. L. *J. Comput. Chem.* **1999**, *20*, 70.
(28) Kaltsoyannis, N. *Chem. Soc. Rev.* **2003**, *32*, 9.
(29) Dognon, J. P. *Coord. Chem. Rev.* **2014**, *266-267*, 110.
(30) Wang, D. Q.; Su, J.; Wu, J. Y.; Li, J.; Chai, Z. F. *Radiochim. Acta* **2014**, *102*, 13.
(31) Wang, C. Z.; Lan, J. H.; Zhao, Y. L.; Chai, Z. F.; Wei, Y. Z.; Shi, W. Q. *Inorg. Chem.* **2013**, *52*, 196.
(32) Becke, A. D. J. *J. Chem. Phys.* **1993**, *98*, 5648.
(33) Lee, C.; Yang, W.; Parr, R. G. *Phys. Rev. B.* **1988**, *37*, 785.
(34) Vukovic, S.; Watson, L. A.; Kang, S. O.; Custelcean, R.; Hay, B. P. *Inorg. Chem.* **2012**, *51*, 3855.
(35) Vallet, V.; Wahlgren, U.; Grenthe, I. *J. Phys. Chem. A* **2012**, *116*, 12373.
(36) Cao, X. Y.; Dolg, M.; Stoll, H. *J. Chem. Phys.* **2003**, *118*, 487.
(37) Cao, X. Y.; Dolg, M. *J. Molec. Struct. (Theochem)* **2004**, *673*, 203.
(38) Kuechle, W.; Dolg, M.; Stoll, H.; Preuss, H. *J. Chem. Phys.* **1994**, *100*, 7535.

(39) Hariharan, P. C.; Pople, J. A. *Theor. Chim. Acta* **1973**, *28*, 213.
(40) Bacskay, G. B. *Chem. Phys.* **1981**, *61*, 385.
(41) Bader, R. F. W. *J. Phys. Chem. A* **1998**, *102*, 7314.
(42) Matta, C. F.; Boyd, R. J. *The Quantum Theory of Atoms in Molecules: From Solid State to DNA and Drug Design*. Wiley-VCH: Weinheim, 2007.
(43) Tassell, M. J.; Kaltsoyannis, N. *Dalton T.* **2010**, *39*, 6719.
(44) Bader, R. F. W. *Atoms in Molecules: A Quantum Theory*. Oxford University Press: Oxford, 1990.
(45) Marenich, A. V.; Cramer, C. J.; Truhlar, D. G. *J. Phys. Chem. B* **2009**, *113*, 6378.
(46) Frisch, M. J.; Trucks, G. W.; Schlegel, H. B.; Scuseria, G. E.; Robb, M. A.; Cheeseman, J. R.; Scalmani, G.; Barone, V.; Mennucci, B.; Petersson, G. A.; Nakatsuji, H.; Caricato, M.; Li, X.; Hratchian, H. P.; Izmaylov, A. F.; Bloino, J.; Zheng, G.; Sonnenberg, J. L.; Hada, M.; Ehara, M.; Toyota, K.; Fukuda, R.; Hasegawa, J.; Ishida, M.; Nakajima, T.; Honda, Y.; Kitao, O.; Nakai, H.; Vreven, T.; Montgomery, J., J. A.; Peralta, J. E.; Ogliaro, F.; Bearpark, M.; Heyd, J. J.; Brothers, E.; Kudin, K. N.; Staroverov, V. N.; Kobayashi, R.; Normand, J.; Raghavachari, K.; Rendell, A.; Burant, J. C.; Iyengar, S. S.; Tomasi, J.; Cossi, M.; Rega, N.; Millam, J. M.; Klene, M.; Knox, J. E.; Cross, J. B.; Bakken, V.; Adamo, C.; Jaramillo, J.; Gomperts, R.; Stratmann, R. E.; Yazyev, O.; Austin, A. J.; Cammi, R.; Pomelli, C.; Ochterski, J. W.; Martin, R. L.; Morokuma, K.; Zakrzewski, V. G.; Voth, G. A.; Salvador, P.; Dannenberg, J. J.; Dapprich, S.; Daniels, A. D.; Farkas, O.; Foresman, J. B.; Ortiz, J. V.; Cioslowski, J.; Fox, D. J. Gaussian 09, Revision C.1; Gaussian, Inc.: Wallingford CT, 2009.
(47) Dennington, R.; Keith, T.; Millam, J. GaussView, Version 5; Semichem Inc.: Shawnee Mission, KS, 2009.
(48) Lu, T.; Chen, F. *J. Comp. Chem.* **2012**, *33*, 580.
(49) Cotton, F. A.; Wilkinson, G.; Gaus, P. L. *Basic Inorganic Chemistry, 2nd Edition*. Wiley: New York, 1987, p 219.
(50) Vallet, V.; Privalov, T.; Wahlgren, U.; Grenthe, I. *J. Am. Chem. Soc.* **2004**, *126*, 7766.
(51) Vallet, V.; Wahlgren, U.; Schimmelpfennig, B.; Szabo, Z.; Grenthe, I. *J. Am. Chem. Soc.* **2001**, *123*, 11999.
(52) Tsushima, S.; Suzuki, A. *J. Mol. Struc. (Theochem)* **2000**, *529*, 21.
(53) Gagliardi, L.; Roos, B. O. *Inorg. Chem.* **2002**, *41*, 1315.
(54) Jensen, M. P.; Nash, K. L. *Radiochim. Acta* **2001**, *89*, 557.
(55) Shamov, G. A.; Schreckenbach, G.; Martin, R. L.; Hay, P. J. *Inorg. Chem.* **2008**, *47*, 1465.
(56) Minasian, S. G.; Keith, J. M.; Batista, E. R.; Boland, K. S.; Clark, D. L.; Conradson, S. D.; Kozimor, S. A.; Martin, R. L.; Schwarz, D. E.; Shuh, D. K.; Wagner, G. L.; Wilkerson, M. P.; Wolfsberg, L. E.; Yang, P. *J. Am. Chem. Soc.* **2012**, *134*, 5586.
(57) Kozimor, S. A.; Yang, P.; Batista, E. R.; Boland, K. S.; Burns, C. J.; Clark, D. L.; Conradson, S. D.; Martin, R. L.; Wilkerson, M. P.; Wolfsberg, L. E. *J. Am. Chem. Soc.* **2009**, *131*, 12125.
(58) Wang, C. C.; Tang, T. H.; Wang, Y. *J. Phys. Chem. A* **2000**, *104*, 9566.
(59) Tian, G. X.; Rao, L. F.; Teat, S. J.; Liu, G. *Chem. Eur. J.* **2009**, *15*, 4172.